ORIGINAL RESEARCH PAPER

Investigation the Synergistic Effect of Adsorption and Photocatalysis for Removal of Dye Pollutants by Hydrogel Supported In$_2$S$_3$ Nanoparticles

Mohammad Reza Mohammad Shafiee[1,*], Janan Parhizkar[2], Sasan Radfar[3]

[1] Department of chemistry Faculty of Sciences, Islamic Azad University– Najafabad Branch, Najafabad, Iran
[2] Nanotechnology Laboratory, Department of Chemistry, University of Isfahan, Isfahan, Iran.
[3] Department of chemistry Faculty of Sciences, Islamic Azad University – Najafabad Branch,Najafabad, Iran

ABSTRACT

Homogenous catalysis which the catalyst operates in the same phase as the reactants is definitely efficient in catalysis processes while it suffers from the impossibility or inconvenience of the catalyst removal from the reaction media. In this research, In2S3 nanoparticles were synthesized by a simple precipitation method and later on immobilized and stabilized in the porous structure as a substrate. The properties of pure hydrogel and In2S3 in hydrogel were characterized by FTIR, DRS, XRD, BET, BJH, FESEM, and EDX. The DRS results confirmed that the stabilization of nanoparticles in hydrogel led to a redshift of the bandgap. The hydrogel with In2S3 indicated a more porous structure in comparison with pure hydrogel. Due to the decrease of bandgap and the increase of specific surface area, In2S3 nanoparticles stabilized in hydrogel removed Rhodamine B (RhB) as a model pollutant very well. The performance of the catalyst in the removal of RhB under dark conditions (adsorption) and visible light irradiation (photocatalysis) was investigated and 77.7% and 95.2% of dye removal percentages were obtained in 120 min under dark and light irradiation, respectively. In conclusion, immobilization In2S3 as a high-efficiency visible light photocatalyst in hydrogel provided a promising heterogeneous and reusable catalyst for water treatment.

Keywords: *Adsorbent, Heterogeneous photocatalyst, Hydrogel, Resorcinol Formaldehyde, water treatment*

INTRODUCTION

Organic pollutants which can cause serious health problems to human beings due to their toxicity and high chemical oxygen demand are widely found in the effluents from petrochemical, textile industries (dyestuffs), and agriculture (pesticides). Different techniques have been employed for the removal of pollutants from aqueous solutions such as physical adsorption, photodegradation, biodegradation, chemical oxidation, etc. The RhB dye is one of the synthetic dyes that are widely used as a colorant in textile and foodstuff industries. It could be harmful and toxic to humans and animals and it could irritate the skin, eyes, and respiratory system [1]. Photocatalytic degradation for dye removal has attracted many attentions due to the utilization of abundant solar energy without the need for additional chemical reagents

Semiconductor photocatalysts are attracting more attention and have become more popular due to their potential applications as efficient photocatalysts in wastewater treatment [2-4]. Semiconductors have different bandgaps. When a photon with an energy that is equal to or greater than a semiconductor bandgap is adsorbed by the

* Corresponding Author Email: *mohammad.r.mohammadshafiee@gmail.com*

semiconductor, an electron will be excited from the valence band to the conduction band, generating a positive hole in the valence band [5]. Electron and hole can generate free radicals able to undergo secondary reactions [6]. Fast recombination of photogenerated charge carriers is a major problem in the photocatalytic process [7].

β-In2S3 is an n-type semiconductor with a narrow bandgap of 2.0-2.3 eV and strong visible absorption. Due to its high photosensitivity and photoconductivity, stable chemical and physical characteristics, and low toxicity, In2S3 indicates a great potential for visible-light-driven photodegradation of water pollutants [8-10].

In_2S_3 has been utilized for dye degradation, water splitting, and solar cell application. It exhibits high dark conductivity due to the presence of the cation or anion vacancies.

The performance of a photocatalyst depends on its chemical and physical structure since it could influence three major stages in photocatalysis; Photon absorption, charge carrier transfers, and catalytic surface reactions [11]. Photocatalysts in different structures as a substrate have been prepared and utilized. Three-dimensional porous structures have a fantastic and effective strategy. Due to their large accessible surface area for adsorption and photoreaction, multi reflection within interconnected open framework and inhibition the aggregation of nanomaterials which exposing more active sites for the catalytic surface reaction they possess high-performance photocatalysis and are the desirable system for supporting nanomaterials [12-13]

Hydrogels are cross-linked polymeric materials with hydrophilic functional groups that are capable of holding large amounts of water in their 3D networks. Hydrogels, over the last years, have been applied to a wide range of utilities such as agriculture, drug delivery system, sealing, coal dewatering, artificial snow, food additives, tissue engineering, biomedical application, etc [14]. Resorcinol formaldehyde hydrogel (RFH) obtained from polycondensation reaction of resorcinol with formaldehyde under alkaline conditions has a dark red color. RFH hydrogels consist of interconnected colloidal like particles and pores filled with liquid. Although in most cases hydrogels are intermediate products in the aerogel or carbogel synthesis process, RFH hydrogels were used as an adsorbent for the removal of chromium (VI) [15]. It seems that RFH is a good choice as a substrate

for the stabilization of nanoparticles due to its porous structure, insolubility in water along with hydrophilicity, and ability to swell in water.

In this study, we synthesized In_2S_3 nanoparticles and later on immobilized them in hydrogel as a porous substrate. The main advantage of hydrogel supported In_2S_3 nanoparticles was to utilize a combination of good photocatalytic property and high interaction surface (provided by In_2S_3 nanoparticles with a porous structure), hydrophilicity, and convenience recyclability which was provided by hydrogel in order to obtain high-performance heterogeneous photocatalyst. The dye removal performance of the pure hydrogel and In_2S_3 nanoparticles stabilized in hydrogel were investigated by the removal of RhB as an organic pollutant in water under dark (adsorption) and visible light (photocatalytic degradation).

MATERIALS AND METHODS
materials
The reagents used in this experiment were of analytical grade and were used without any further purification. Indium (III) chloride ($InCl_3$), sodium sulfide nonahydrate ($Na_2S_3.9H_2O$), RhB (C.I.45170), resorcinol ($C_6H_6O_2$), Formaldehyde (CH_2O), and Sodium Carbonate (Na_2CO_3) were analytically pure and from sigma Aldrich Co.

synthesis of In_2S_3
To prepare In_2S_3 nanoparticles, first, 0.01 M $InCl_3$ ethanol-water solution (1:1 v/v) was prepared and later on stirred over magnetic stirrer. 0.03 M Na_2S solution in the ethanol-water mixture (1:1 v/v) was prepared and slowly added to the $InCl_3$ solution under constant stirring and was kept for 2 h. The mixture was centrifuged, precipitated, and washed three times with distilled water and ethanol and later on, was dried at 120ºC for 12 h. Ethanol was used as a solvent due to make a dispersing medium and preventing agglomeration during the growth process [16-17].

synthesis of hydrogel
Resorcinol formaldehyde (RF) hydrogel was synthesized by the polycondensation of resorcinol and formaldehyde in the presence of Na_2CO_3 as the basic catalyst. Distilled water was used as a diluent [18]. 9.91g resorcinol and 0.0318g Na_2CO_3 (R/C=300) were mixed and later on dissolved in 18.8 ml distilled water. The solution was heated to 70ºC under magnetic stirring in a sealed flask. In another flask, 13.5 ml of formaldehyde (37 wt. % in Water,

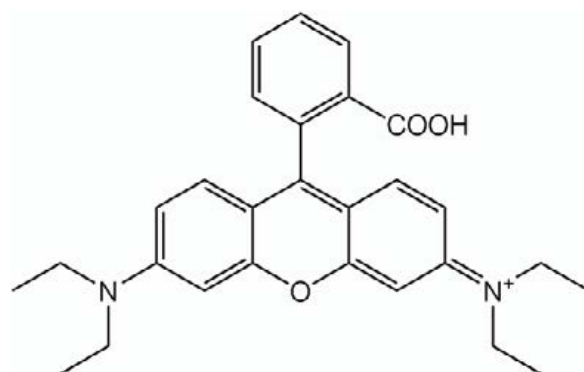*J. Water Environ. Nanotechnol., 5(4): 358-368 Autumn 2020*

359

Fig.1. Chemical structure of Rhodamine B

stabilized by 10-15 wt. % Methanol) was heated to 70°C. The solutions of the two mentioned flasks were mixed. Subsequently, the solution was divided equally into sample holders with diameter and height equal to 13 and 20 mm, respectively. Later on, each sample holder was sealed with paraffin film and the solutions were put in the oven at 70°C for 120 min (gelation time).

synthesis of hydrogel supported In$_2$S$_3$ composite

In order to synthesize In$_2$S$_3$ stabilized in a hydrogel, 10 mg of In$_2$S$_3$ nanoparticles per 1 ml of the Resorcinol-formaldehyde mixture (before solution gelation) were added to the abovementioned system and the mixture stirred for 4 min and after casting in sample holders were put in the oven at 70°C for 120 min.

characterization

X-ray diffraction patterns (XRD) of samples recorded at room temperature using D8Advance, BRUKER, using CuKα radiation, and 2Θ=5-80°. Diffuse reflectance spectra (DRS) were collected with a V-670, JASCO spectrophotometer and transformed into the absorption spectra according to the Tauc relationship. The infrared spectra were obtained on an FT-IR 6300 using KBr as the reference sample within a wavelength range of 400 – 4000 cm^{-1}. The morphologies of the sample were obtained by field emission scanning electron microscopy (FESEM) of the scientific England agar company. The Branauer-Emmet-Teller (BET) specific surface area and Barrett-Joyner-Halenda (BJH) pore structure of the samples were characterized by nitrogen adsorption at 77K with a micrometric BEIOSORP Mini from Microtrac Bel Crop.

photocatalytic and adsorption behavior of nanocomposites to removal RhB

A stock solution of RhB was prepared and standard diluted solutions of RhB (0.5, 1, 2, 3, and 4 ppm) were prepared from the stock solution by dilution. Fig.1 illustrates the chemical structure of RhB. The absorption intensity of each solution was evaluated in λ$_{max}$ with a UV-Vis spectrometer. The calibration curve of RhB was drawn and a linear correlation between intensity and concentration was obtained. In order to investigate adsorption capacity, the hydrogel was put in 25 ml of 3 ppm RhB solution in a petri dish while the solution stirring in a dark place. In determining interval times (10 min) the hydrogel was removed from the solution and the concentration of RhB was monitored till 120 min. To investigate the photocatalytic performance of hydrogel, conditions (the volume and concentration of RhB solution) were similar to adsorption investigation except for the application of ultraviolet radiation to hydrogel during its performance in order to remove RhB from solution. RhB concentration changes in this step represented the synergistic effect of adsorption and photocatalytic properties. These experiments were done with hydrogel supported In$_2$S$_3$ composite.

RESULT AND DISCUSSION
FTIR

Fig.2. indicates the FT-IR spectra of as-prepared adsorbents and catalysts. In the FTIR spectrum of the hydrogel, the broadband at 3428 cm^{-1} could be related to two sources: a) OH groups bonded to the benzene ring and b) –CH$_2$OH groups of resorcinol molecules which did not contribute to the network formation. The bands at 2938 cm^{-1} and 1469 cm^{-1} are referred to –CH$_2$ bond stretching vibrations.

360

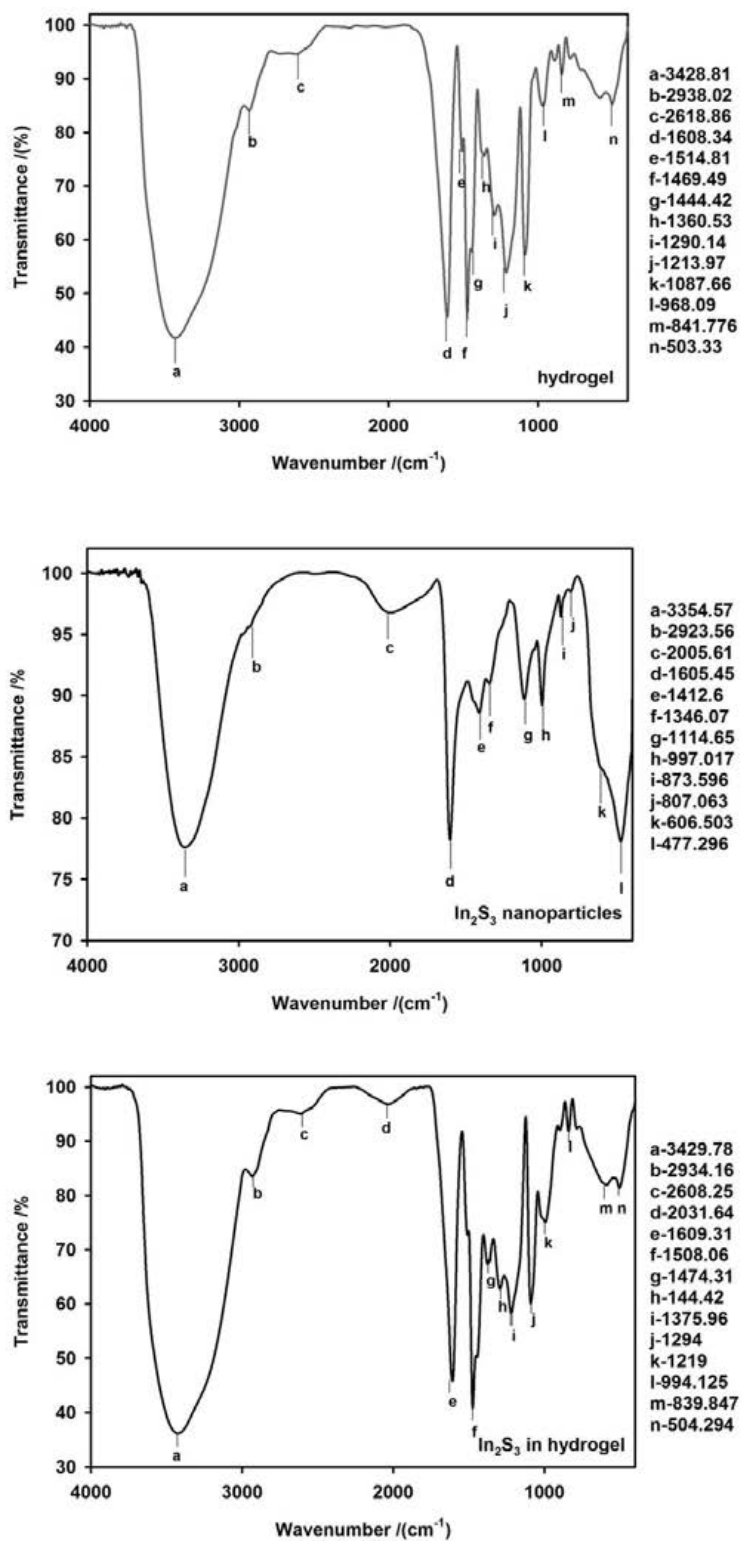J. Water Environ. Nanotechnol., 5(4): 358-368 Autumn 2020

a-3428.81
b-2938.02
c-2618.86
d-1608.34
e-1514.81
f-1469.49
g-1444.42
h-1360.53
i-1290.14
j-1213.97
k-1087.66
l-968.09
m-841.776
n-503.33

hydrogel

a-3354.57
b-2923.56
c-2005.61
d-1605.45
e-1412.6
f-1346.07
g-1114.65
h-997.017
i-873.596
j-807.063
k-606.503
l-477.296

In$_2$S$_3$ nanoparticles

a-3429.78
b-2934.16
c-2608.25
d-2031.64
e-1609.31
f-1508.06
g-1474.31
h-144.42
i-1375.96
j-1294
k-1219
l-994.125
m-839.847
n-504.294

In$_2$S$_3$ in hydrogel

Fig.2. FTIR spectra of hydrogel, In$_2$S$_3$ nanoparticles, In$_2$s$_3$ immobilized in hydrogel.
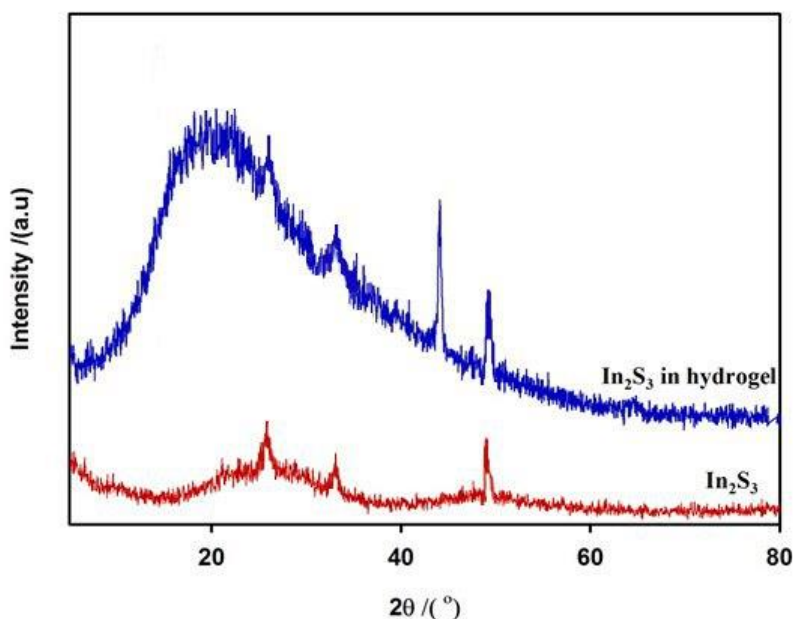
Fig.3. XRD patterns of Hydrogel and In$_2$s$_3$ immobilized in hydrogel.

Table 1. Specific surface area, pore volume and pore diameter of hydrogel and In$_2$S$_3$ in hydrogel

Sample	S_{BET} (m^2.g^{-1})	Pore volume (cm^3.g^{-1})	Mostly pore diameter By BJH (nm)
Hydrogel	10.066	0.0040829	2.52
In$_2$S$_3$ in hydrogel	241.24	0.1194	3.48

The aromatic ring stretching peak is revealed at 1608 cm^{-1}. The bands at 1290 cm^{-1} and 1087 cm^{-1} are related to C-O-C linkage stretching which results from the polycondensation reaction between resorcinol and formaldehyde [19].

In the FT-IR spectrum of In$_2$S$_3$ nanoparticles, the peak at 807 cm^{-1} is due to the bonding of In-S. [20].

The presence of Na$_2$S in the product is indicated by the peak observed in the FTIR spectrum at 477 cm^{-1}. It is clearly illustrated by a comparison of the FTIR spectrum with the Na$_2$S IR spectrum in the SDBS database (SDBS-no: 40243). In the FTIR spectrum of In$_2$S$_3$ in the hydrogel, there are no related peaks of In$_2$S$_3$ and the spectrum is very similar to the hydrogel spectrum due to the small amounts of In$_2$S$_3$ nanoparticles.

XRD

Fig.3. shows XRD patterns of In$_2$S$_3$ nanoparticle, In$_2$S$_3$ in the hydrogel. The appearance of the X-ray pattern diffraction is very similar to the X-ray pattern of cubic phase β- In$_2$S$_3$ (JCPDS NO.65-0459) [21]. The diffraction peaks at 26, 33, and 49.2 correspond to (311), (400), and (440) planes of In$_2$S$_3$. In the In$_2$S$_3$ in hydrogel XRD pattern, the amorphous phase is available that could be attributed to the hydrogel. Besides, an intensive peak at 44° is matched by the most intensive peak of carbon in the diamond phase (JCPDS NO.01-075-0409). Moreover, the peaks of In$_2$S$_3$ have appeared in the XRD pattern of In$_2$S$_3$ in the hydrogel.

BET

The specific surface area and pore volume and size of the samples were measured by BET and BJH respectively. These data are summarized in Table 1. BET surface area (S_{BET}) of the hydrogel, In$_2$S$_3$ in hydrogel are 10.066, 241.24 m^2.g^{-1} respectively; indicating all samples had porous structure. The higher S_{BET} value indicates a more porous structure of the samples. In other words, a more porous structure provides more surface area and subsequently more active sites for interaction between adsorbent and pollutants. Results confirmed that the addition of nanomaterials
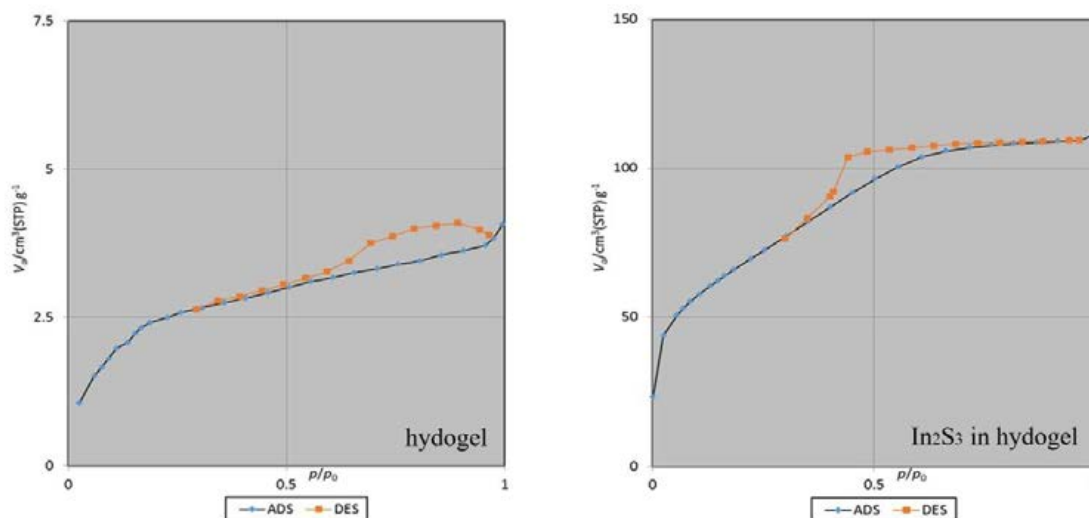
Fig.4. N$_2$ Adsorption-desorption isotherms of hydrogel and In$_2$S$_3$ immobilized in hydrogel

Table 2. Kinetic parameters of RhB removal using In$_2$S$_3$ in hydrogel

name	Adsorption %	Photocatalytic %	Photocatalytic + adsorption%	K$_1$(min⁻¹)	R²
In₂S₃ in hydrogel	77.7%	17.5%	95.2%	0.0262	0.9975

increased the specific surface area of the hydrogel. This is in accordance with the results of our previous work [19] The lowest value of pore volume was measured for pure hydrogel (0.00408 cm³.g⁻¹). The BET results suggested that the presence of In$_2$S$_3$ nanoparticles improved the porosity of hydrogel and increased the specific surface area up to twenty-four times. Furthermore, the results indicated that the presence of nanomaterial in the hydrogel synthesis procedure had a better effect on porosity. The most probable pore diameters for the above-mentioned samples measured by BJH were between 2.52 and 3.48 nm. The N$_2$ adsorption-desorption isotherms of the sample are shown in Fig.4. The shape of the hysteresis loop could be used to understand the morphology of pore shape in solid. The adsorption/desorption isotherms of the samples belong to type IV (isotherm with hysteresis loop) according to IUPAC. Such an isotherm type indicates that samples contain meso size pores. The hysteresis loops of samples indicate disorder structure with bottleneck pores [22]. Table 1 summarizes the specific surface area (BET), pore-volume, and mostly pore diameter by BJH of hydrogel and In$_2$S$_3$ in the hydrogel.

DRS

The photocatalytic performance of the catalysts

is dependent on light absorption and charge separation ability. The optical absorption of In$_2$S$_3$ nanoparticles and In$_2$S$_3$ immobilized in hydrogel were recorded using a UV-vis spectrometer and are illustrated in Fig.5. The absorbance edge of In$_2$S$_3$ nanoparticles located at around 650 nm and the bandgap energy calculated from Tauc relation was approximately 2 eV. This nanomaterial when immobilized in hydrogel exhibited the shift of absorbance edge to a longer wavelength. As a result, the bandgap energy of In$_2$S$_3$ nanoparticles in hydrogel shifted to lower energy (redshift) and was calculated from Tauc plot 1.4 eV. There are two possible reasons for this redshift: first, In$_2$S$_3$ nanoparticles have interactions with OH groups of the resorcinol formaldehyde hydrogel that leads to the decrease of bandgap and subsequently makes the redshift. Second, the presence of In$_2$O$_3$ as a byproduct of In$_2$S$_3$ synthesis could interfere with the energy levels of In$_2$S$_3$ which results in a smaller bandgap and a redshift. Precise determination of the reason for redshift needs more analysis and investigation. The result from DRS implied that the photocatalyst had photocatalytic activity in the range of visible light.
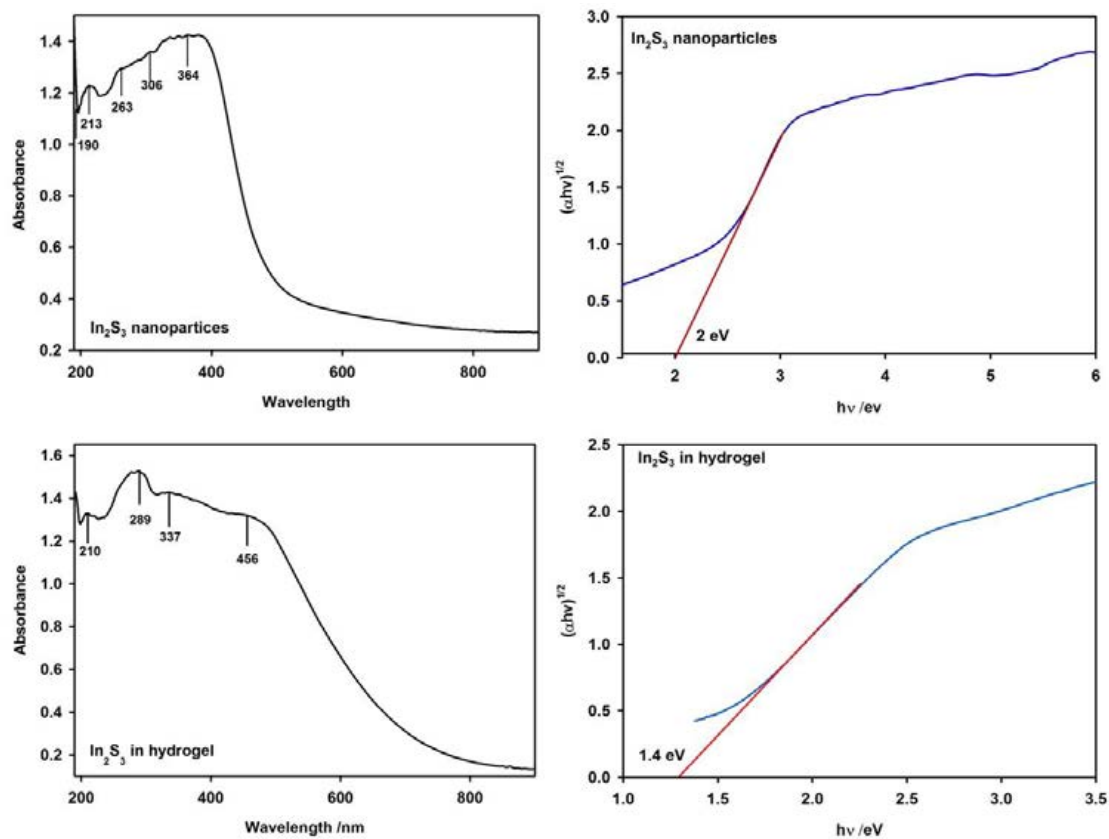
FESEM/EDS

The morphology and the elements of the

J. Water Environ. Nanotechnol., 5(4): 358-368 Autumn 2020

363

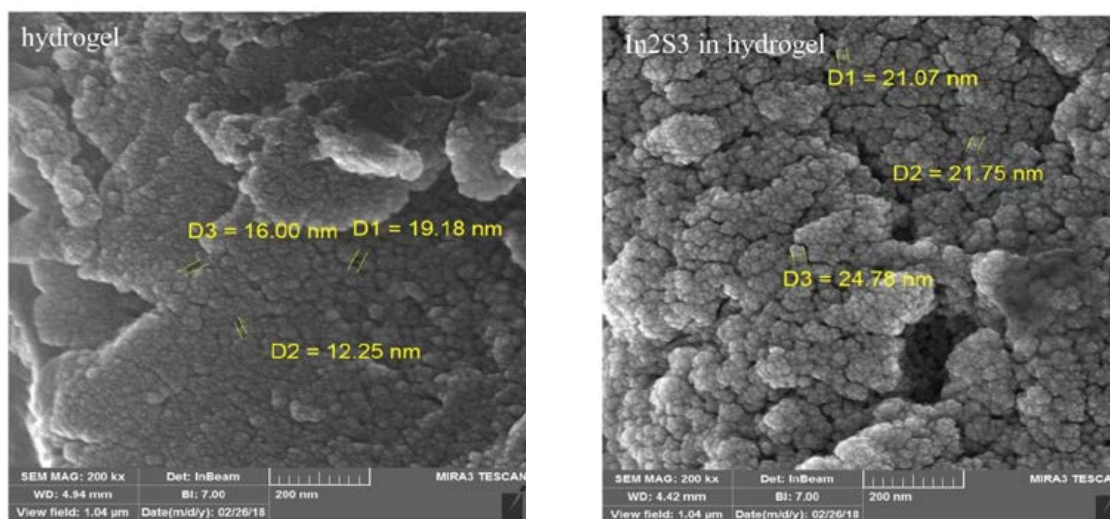Fig.5. UV-Vis absorption spectra and Tauc plots of In₂S₃ nanoparticles and In₂s₃ immobilized in hydrogel.

Fig.6. FESEM images of hydrogel and In₂s₃ immobilized in hydrogel.

sample were investigated with SEM and EDX, respectively. SEM pictures of samples are shown in Fig.6. The hydrogel structure is affected by the

presence of In₂S₃ nanoparticles so that hydrogel with nanomaterials indicated a cauliflower shape and more pores in structure. The particles in the
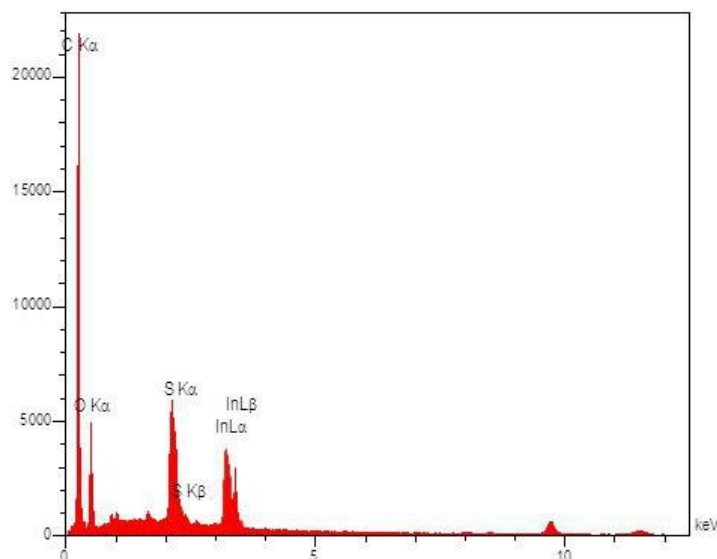
364

J. Water Environ. Nanotechnol., 5(4): 358-368 Autumn 2020
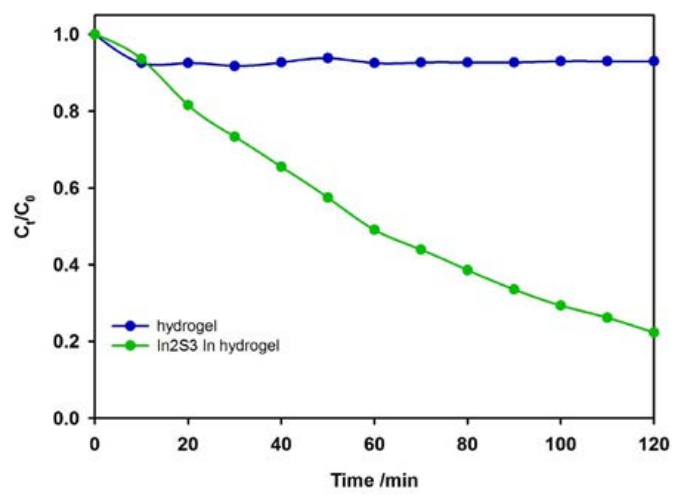
Fig.7. the EDX pattern of In₂s₃ immobilized in hydrogel.

Fig.8. Removal of RhB over hydrogel and In₂s₃ immobilized in hydrogel under dark (adsorption).

composite are larger than pure hydrogel generally. The semi-quantitative analysis was carried out by using the EDX technique for samples. Fig.7 shows the EDX pattern with relative analysis for the samples. The results confirm the existence of In_2S_3 nanoparticles in the hydrogel.

adsorption and photocatalytic study

The photocatalytic activity of samples was pointed out by evaluating the photodegradation of RhB under visible light irradiation. The first step of degradation is the adsorption of pollutants on the surface of the adsorbent. Due to the importance of adsorption, adsorption investigation was done

in the dark (Fig.8). In order to investigate the photodegradation of the RhB over samples, visible light was provided by 4 counts of 8 W fluorescent lamp. The changes of RhB solution concentration is presented in Fig.9. The percentage of adsorption and adsorption/photocatalytic synergy was obtained by this equation:

$$\%R = \frac{C_0 - Ce}{C_0} \times 100$$

Where C_0 is the initial concentration of the dye and C_e is the equilibrium concentration of dye and R is the percentage of dye removal.
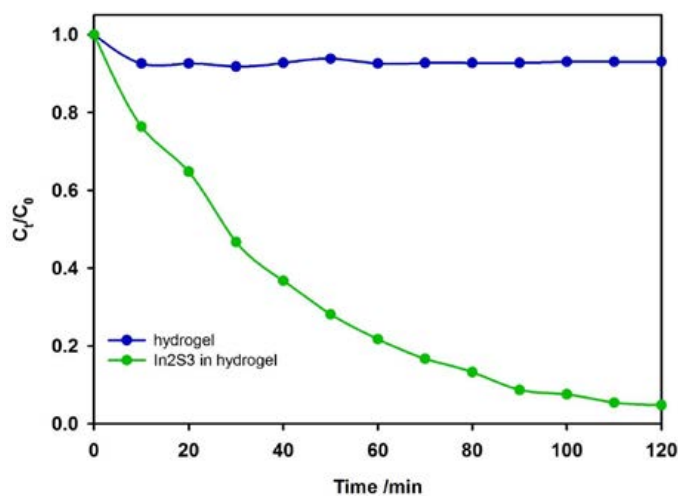
J. Water Environ. Nanotechnol., 5(4): 358-368 Autumn 2020

365

Fig.9. Removal of RhB over hydrogel and In$_2$s$_3$ immobilized in hydrogel under light irradiation (adsorption and photodegradation).
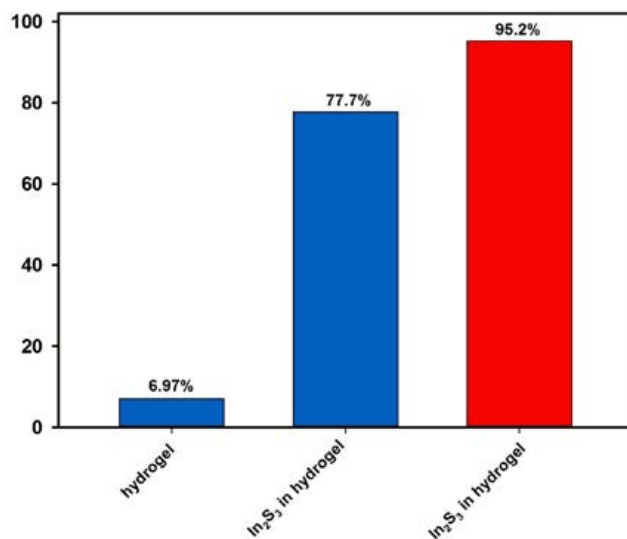

Fig.10. Removal percentage of RhB over hydrogel, In$_2$s$_3$ immobilized in hydrogel in dark and light irradiation condition after 120 min

For the RF hydrogel after 2h of placing it in the dark condition, 6.97% of RhB removal was achieved. The absorbance of RhB solution indicated 77.7% removal under the dark condition and 95.2% under visible light for In$_2$S$_3$ nanoparticles in hydrogel (Fig.10). As we can see the results indicate the adsorption efficiency of hydrogel was improved dramatically with the presence of nanomaterials. It could be attributed to the large specific surface of nanomaterials and the more porosity of hydrogel with nanoparticles stabilized in them which possess significant amounts of sites for interaction between RhB solution and adsorbent. The pure

photodegradation percentages of the samples were calculated by subtracting the removal percentage under dark from the removal percentage under visible light. Regarding these calculations, the photocatalytic contribution percentage of In$_2$S$_3$ nanoparticles in the hydrogel is equal to 17.5%. The good performance of In$_2$S$_3$ nanoparticles in hydrogel could be attributed to two main reasons: 1- low bandgap of In$_2$S$_3$ nanoparticles which easily made electron-hole pair and then they can degrade the adsorbed dyes on the surface of the nanoparticle. 2- Strong adsorption of RhB in In$_2$S$_3$ nanoparticles in the hydrogel is the first step for photodegradation
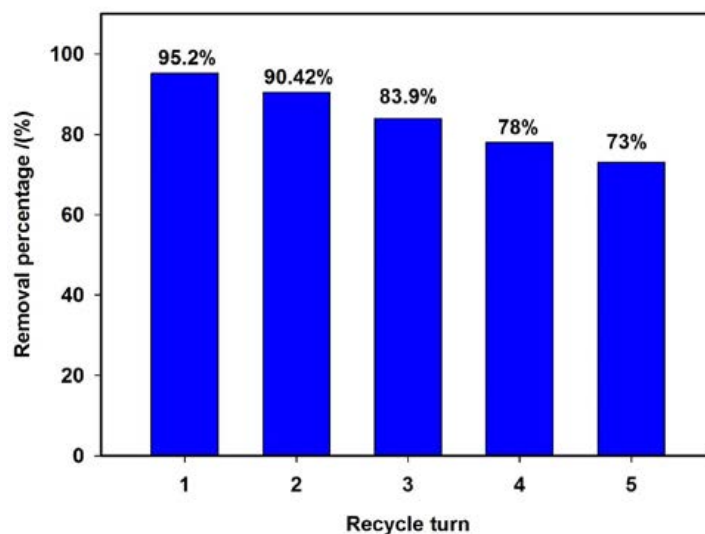
366

J. Water Environ. Nanotechnol., 5(4): 358-368 Autumn 2020

Fig.11.cycling runs of In₂s₃ immobilized in hydrogel for removal of RhB under visible light irradiation.

of dye. Due to the best performance of In$_2$S$_3$ in the hydrogel in the RhB removal, it was used to degrade the RhB solution (3 ppm) under light irradiation for 5 times in order to evaluate the catalytic stability and recyclability. The irradiation time was 120 min and after each experiment, the concentration of RhB was determined. The results were represented in Fig.11. As the removal percentage indicates the catalyst (In$_2$S$_3$ in hydrogel) has significant efficiency after 5 turn photocatalytic processes. The catalyst shows good chemical stability and reusability. The low decrease of the removal percentage after each photocatalytic process could be attributed to the occupation of the interaction sites by the dye. It should be noted that the heterogeneous photocatalyst was used for the next dye removal process without any treatment or desorption actions. The degradation kinetics of RhB using hydrogel, In$_2$S$_3$ in the hydrogel was evaluated by first and second-order rate equations (eq.1&2).

$$\ln \frac{C_t}{C_0} = -k_1 t \qquad \text{eq.1}$$

$$\left(\frac{1}{C_t} \right) = \left(\frac{1}{C_0} \right) + k_2 t \qquad \text{eq.2}$$

Where C_0 is the initial concentration of RhB dye solution, C_t is the concentration of RhB dye solution at time t, k_1 is the first-order constant, k_2 is the second-order rate kinetic, t is the irradiation time. Both type plots have been drawn and the regression correlation coefficient (R^2) was achieved and it shows that R^2 of first-order plots are closer to 1. The kinetic of RhB is going to follow the first-order kinetic rate.

CONCLUSION

Resorcinol formaldehyde hydrogel (substrate), In$_2$S$_3$ nanoparticles (photocatalyst), and In$_2$S$_3$ nanoparticles stabilized in hydrogel were synthesized and characterized by FTIR, DRS, XRD, BET, FESEM techniques. The dye removal performance of hydrogel supported In$_2$S$_3$ nanoparticles in the dark and under light exposure was evaluated. We have demonstrated an effective method in order to make heterogeneous photocatalysts in the porous 3D hydrogel. The stabilization of In$_2$S$_3$ nanoparticles in resorcinol formaldehyde hydrogel shifted the band edge to longer wavelengths and the mutual presence of nanoparticles improved the porosity of hydrogel. These two reasons led to the good performance of In$_2$S$_3$ nanoparticles stabilized in the hydrogel in the dye removal from water (about 95%). This research indicates the potential application of resorcinol formaldehyde hydrogel as a porous substrate to immobilize photocatalytic nanoparticles.

J. Water Environ. Nanotechnol., 5(4): 358-368 Autumn 2020

367

CONFLICT OF INTEREST

The authors declare that they have no conflict of interest.

REFERENCES

1. Martínez-Huitle CA, Brillas E. Decontamination of wastewaters containing synthetic organic dyes by electrochemical methods: A general review. Applied Catalysis B: Environmental. 2009;87(3-4):105-45.

2. Chen C, Ma W, Zhao J. Semiconductor-mediated photodegradation of pollutants under visible-light irradiation. Chemical Society Reviews. 2010;39(11):4206.

3. Legrini O, Oliveros E, Braun AM. Photochemical processes for water treatment. Chemical Reviews. 1993;93(2):671-98.

4. Lee KM, Lai CW, Ngai KS, Juan JC. Recent developments of zinc oxide based photocatalyst in water treatment technology: A review. Water Research. 2016;88:428-48.

5. Linsebigler AL, Lu G, Yates JT. Photocatalysis on TiO2 Surfaces: Principles, Mechanisms, and Selected Results. Chemical Reviews. 1995;95(3):735-58.

6. Turchi, C. S., & Ollis, D. F. (1990). Photocatalytic degradation of organic water contaminants: mechanisms involving hydroxyl radical attack. *Journal of catalysis*, *122*(1), 178-192.

7. Rossetti R, Brus L. Electron-hole recombination emission as a probe of surface chemistry in aqueous cadmium sulfide colloids. The Journal of Physical Chemistry. 1982;86(23):4470-2.

8. Fu X, Wang X, Chen Z, Zhang Z, Li Z, Leung DYC, et al. Photocatalytic performance of tetragonal and cubic β-In2S3 for the water splitting under visible light irradiation. Applied Catalysis B: Environmental. 2010;95(3-4):393-9.

9. He Y, Li D, Xiao G, Chen W, Chen Y, Sun M, et al. A New Application of Nanocrystal In2S3 in Efficient Degradation of Organic Pollutants under Visible Light Irradiation. The Journal of Physical Chemistry C. 2009;113(13):5254-62.

10. Liu G, Jiao X, Qin Z, Chen D. Solvothermal preparation and visible photocatalytic activity of polycrystalline β-In2S3nanotubes. CrystEngComm. 2011;13(1):182-7.

11. Kerc A, Bekbolet M, Saatci AM. Effects of oxidative treatment techniques on molecular size distribution of humic acids. Water Science and Technology. 2004;49(4):7-12.

12. Sharma RK, Chouryal YN, Chaudhari S, Saravanakumar J, Dey SR, Ghosh P. Adsorption-Driven Catalytic and Photocatalytic Activity of Phase Tuned In2S3 Nanocrystals Synthesized via Ionic Liquids. ACS Applied Materials & Interfaces. 2017;9(13):11651-61.

13. Wang X, Liang Y, An W, Hu J, Zhu Y, Cui W. Removal of chromium (VI) by a self-regenerating and metal free g-C3N4/graphene hydrogel system via the synergy of adsorption and photo-catalysis under visible light. Applied Catalysis B: Environmental. 2017;219:53-62.

14. Ahmed EM. Hydrogel: Preparation, characterization, and applications: A review. Journal of Advanced Research. 2015;6(2):105-21.

15. Mulani K, Patil V, Chavan N, Donde K. Adsorptive removal of chromium(VI) using spherical resorcinol-formaldehyde beads prepared by inverse suspension polymerization. Journal of Polymer Research. 2019;26(2).

16. Kokane SB, Sasikala R, Phase DM, Sartale SD. In2S3 nanoparticles dispersed on g-C3N4 nanosheets: role of heterojunctions in photoinduced charge transfer and photoelectrochemical and photocatalytic performance. Journal of Materials Science. 2017;52(12):7077-90.

17. Ghosh SK, Deguchi S, Mukai S-a, Tsujii K. Supercritical EthanolA Fascinating Dispersion Medium for Silica Nanoparticles. The Journal of Physical Chemistry B. 2007;111(28):8169-74.

18. Horikawa T, Hayashi Ji, Muroyama K. Controllability of pore characteristics of resorcinol–formaldehyde carbon aerogel. Carbon. 2004;42(8-9):1625-33.

19. Shafiee MRM, Parhizkar J, Radfar S. Removal of Rhodamine B by g-C3N4/Co3O4/MWCNT composite stabilized in hydrogel via the synergy of adsorption and photocatalysis under visible light. Journal of Materials Science: Materials in Electronics. 2019;30(13):12475-86.

20. Huang, N. M. (2011). Synthesis and characterization of in 2S 3 nanorods in sucrose ester water-in-oil microemulsion. *Journal of Nanomaterials (JNM),* 2011, 1-6.

21. Shi Y, Yang Y-L, Fan R-Q, Li L, Yu J, Li S. Self-assembled synthesis and surface photovoltage properties of polyhedron-constructed micrometer solid sphere and hollow-sphere In2S3. RSC Adv. 2014;4(33):17245-8.

22. Liu X, Xiong J, Liang L. Investigation of pore structure and fractal characteristics of organic-rich Yanchang formation shale in central China by nitrogen adsorption/desorption analysis. Journal of Natural Gas Science and Engineering. 2015;22:62-72.

368

J. Water Environ. Nanotechnol., 5(4): 358-368 Autumn 2020